JOURNAL OF
biomaterials applications

Article

Journal of Biomaterials Applications
28(3) 434–447

DOI: 10.1177/0885328212459777
jba.sagepub.com
SAGE

Self-assembled photosensitizer-conjugated nanoparticles for targeted photodynamic therapy

Linlin Zhao[1], Tae-Hyun Kim[2,3], Kang Moo Huh[4], Hae-Won Kim[2,3] and So Yeon Kim[1,5]

Abstract

An effective tumor-targeted drug delivery system for photodynamic therapy was developed by designing ligand-mediated nanoparticles with stable formulations of a hydrophobic photosensitizer. Novel folic acid (FA)-conjugated amphiphilic block copolymers of polyethylene glycol (PEG) and poly-β-benzyl-L-aspartate (PBLA) with the potential to act as pH-responsive drug release reservoirs were synthesized. The photosensitizer, 2,4-diacetyl deuteroporphyrin IX dimethyl ether (DD-PpIX), was conjugated to the copolymers through pH-sensitive hydrazone linkage. The syntheses and compositions of all copolymers were confirmed by ^{1}H NMR measurement. Photosensitizer-conjugated amphiphilic copolymeric nanoparticles (FA-PEG-P(Asp-Hyd)-DD-PpIX) were prepared by micelle formation in aqueous solution. The particle sizes of the FA-PEG-PBLA and FA-PEG-P(Asp-Hyd)-DD-PpIX nanoparticles were determined by light-scattering measurements. The range was 105–298 nm, depending on copolymer molecular weight and composition. Field emission scanning electron microscopy showed that the FA-PEG-P(Asp-Hyd)-DD-PpIX copolymeric nanoparticles were submicron in size and spherical in shape. The results of in vitro release tests showed that the release profiles of DD-PpIX from the nanoparticles were strongly pH-dependent and influenced by the amount of photosensitizer that was conjugated. In vitro tests using HeLa cells indicated that the FA-PEG-P(Asp-Hyd)-DD-PpIX nanoparticles had low dark-toxicity and showed more than 97% of cellular uptake. Based on our results, the FA-PEG-P(Asp-Hyd)-DD-PpIX nanoparticle system could be a promising approach for developing novel photosensitizer delivery carriers for photodynamic therapy.

Keywords

Nanoparticle, photodynamic therapy, drug delivery system, polyethylene glycol, poly-β-benzyl-L-aspartate

Introduction

Photodynamic therapy (PDT) is increasingly recognized as a promising treatment for a variety of oncological, cardiovascular, dermatological, and ophthalmic diseases.[1,2] PDT is based on the use of photosensitizers (PS) that are preferentially taken up and retained by diseased tissue. Upon photoactivation with visible light at appropriate wavelengths, the generation of cytotoxic species such as reactive singlet oxygen ($^1O_2$) leads to irreversible destruction of tissues.[3–8] Compared to current treatments including surgery, radiation therapy and chemotherapy, PDT is an effective and selective method of destroying diseased tissue without damaging surrounding healthy tissues. However, a problem limiting the use of many current PS is the difficulty of preparing pharmaceutical formulations for parenteral administration. Because of their low water solubility, hydrophobic PS cannot be directly injected intravenously.[9,10]

To overcome these problems, various strategies have been employed to prepare stable formulations of hydrophobic PS. Conjugation to water-soluble

[1]Graduate School of Green Energy Technology, Chungnam National University, South Korea
[2]Department of Nanobiomedical Science and WCU Research Center, Dankook University, South Korea
[3]Institute of Tissue Regeneration Engineering (ITREN), Dankook University, South Korea
[4]Department of Polymer Science and Engineering, College of Engineering, Chungnam National University, South Korea
[5]Department of Chemical Engineering Education, College of Education, Chungnam National University, South Korea

Corresponding author:
So Yeon Kim, Department of Chemical Engineering Education, College of Education, Chungnam National University, South Korea.
Email: kimsy@cnu.ac.kr

polymers or encapsulation in colloidal carriers such as oil-in-water emulsions,[11] liposomes,[12] ceramic-based nanoparticles,[13] gold nanoparticles,[14] polymer nanoparticles,[15] and polymeric micelles[16] have shown potential for successful delivery.

Among these systems, self-assembled amphiphilic block polymeric nanoparticles have gained interest as drug delivery systems for hydrophobic drugs, including PS. They are small in size, and exhibit thermodynamic and kinetic stability in vivo, high drug-loading capacity, and good biocompatibility. When systemically injected, they exhibit prolonged circulation and avoid rapid renal clearance and unwanted uptake by the reticuloendothelial system (RES). This results in enhanced permeability and retention (EPR) in tumor tissues with defective vascular architecture.[17] The block copolymers are composed of hydrophilic and hydrophobic segments. In an aqueous environment, the hydrophobic segment of the copolymer forms the hydrophobic core of a nanoparticle by hydrophobic interaction, while the hydrophilic segment forms the outer shell. The hydrophobic nanoparticle core serves as a nanoenvironment for the incorporation of hydrophobic drugs such as PS, while the outer shell serves as a stabilizing interface between the hydrophobic core and the external medium. Stimuli-responsive polymeric nanoparticles show even more specific delivery to target sites through controlled release by reactions to stimuli such as temperature or pH.[18–22] Interstitial fluid in tumors is known to have a lower pH (pH 6.75) than normal tissues (pH 7.23). In addition, if internalized by endocytosis, nanoparticles are found in the acidic environments of endosomes and lysosomes (pH 5.0–5.5). If such environments accelerate degradation of pH-sensitive nanoparticles, the drug is released. Therefore, the application of pH-sensitive nanoparticles may overcome the intracellular barriers of endosomal or lysosomal membranes that prevent drugs from reaching their targets.

Polyethylene glycol (PEG), a non-toxic, water-soluble polymer, is approved by the FDA for internal use. Importantly, it prevents protein adsorption (opsonization) and cellular adhesion, therefore preventing RES uptake of nanoparticles.[23] Hydrophobic poly(β-benzyl-L-aspartate) (PBLA) is a biocompatible and biodegradable polymer-like protein. The side chains of PBLA can be activated or chemically modified to introduce functional groups and conjugate drugs. Folic acid (FA) has become an attractive candidate molecule for targeting cancer cells because it is an essential vitamin for nucleotide base biosynthesis and is taken up in elevated quantities by proliferating cells. The receptor for FA is overexpressed in many human cancers, including malignancies of the ovary, brain, kidney, breast, myeloid cells, and lung.[24–26]

The main objective of this study was to develop an effective tumor-targeted PS delivery system with pH-sensitive cleavage linkages for photodynamic therapy. We synthesized FA-conjugated amphiphilic block copolymers composed of PEG and PBLA. The PS 2,4-diacetyl deuteroporphyrin IX dimethyl ether (DD-PpIX), which is a derivative of porphyrin and an effective hydrophobic PS for PDT, was conjugated to the side chain of the core-forming segment via an acid-labile hydrazone bond that is stable at physiological pH (7.0–7.4) but degraded at the lower pH (5.0–5.5) of the endosomal/lysosomal compartments. The polymeric nanoparticles were prepared by micelle formation in an aqueous solution. The molecular weights and chemical compositions of the copolymers were determined by ^{1}H NMR. The particle size, size distribution, and morphology were determined and in vitro release profiles of DD-PpIX from the nanoparticles under different pH conditions were investigated. In vitro cellular localization was investigated in HeLa cells by confocal microscope and flow cytometry. The phototoxicity of free DD-PpIX and FA-PEG-P(Asp-Hyd)-DD-PpIX nanoparticles was also investigated.

Materials and methods

Materials

FA, PEG-bis(amine) (molecular weight: 3.350 kDa), β-benzyl-L-aspartate (BLA), triethylamine (TEA), hydrazine monohydrate, and sodium bicarbonate were purchased from Sigma Chemical Co. (St. Louis, MO, USA). Triphosgene was purchased from Aldrich Chemical Co. (Milwaukee, WI, USA). N-hydroxysuccinimide (NHS) and N,N′-dicyclohexylcarbodiimide were purchased from Fluka (Buchs, Switzerland). Dimethyl sulfoxide (DMSO), tetrahydrofuran (THF), n-hexane, benzene, N,N-dimethylformamide (DMF), chloroform, diethyl ether, 1,4-dioxane, methanol, and acetic acid were purchased from Samchun Pure Chemical Co., Ltd. (Gyeonggi-do, Korea), and 2,4-diacetyl deuteroporphyrin IX dimethyl ether (DD-PpIX) was purchased from Frontier Scientific, Inc. (Logan, UT, USA). Spectra/Por membranes were purchased from Spectrum Laboratories, Inc. (Rancho Dominguez, CA, USA). RPMI 1640 medium, Dulbecco's modified Eagle's medium (DMEM), fetal bovine serum (FBS), penicillin, streptomycin, and Dulbecco's phosphate buffered saline (DPBS) were purchased from GibcoBRL (Invitrogen Corp., CA, USA). All other chemicals were of analytical grade and used as received without further purification.

Synthesis of photosensitizer-conjugated amphiphilic block copolymers

Synthesis of folic acid–PEG-NH_2 (FA-PEG-NH_2). FA (113 mg; 0.25 mmol) was dissolved completely in DMSO (6 mL), and NHS (37 mg; 0.32 mmol), N,N′-dicyclohexylcarbodiimide (66 mg; 0.32 mmol), PEG-bis(amine) (714.8 mg; 0.21 mmol) and TEA (170 μL; 2.1 mmol) were added. The reaction mixture was stirred at 400 r/min for 24 h at room temperature in the dark under nitrogen. The mixture was diluted with 18 mL of deionized water and the by-product, dicyclohexylurea, was removed by filtration.[27–29] The product was purified by dialysis against a $NaHCO_3$ solution (pH 8.4) for 2 days to remove unconjugated FA, dialyzed against deionized water to remove $NaHCO_3$, and freeze-dried.

Preparation of β-benzyl-L-aspartate N-carboxy anhydride (BLA-NCA). BLA (7.2 g; 32.3 mmol) was added to a round-bottom flask. Triphosgene (4.3 g; 14.5 mmol) dissolved in anhydrous THF (70 mL) was added slowly. The reaction mixture was stirred at 60°C under nitrogen for 2 h. The mixture became clear during the reaction. The solvent of reactant mixture was removed using a rotary evaporator and the product was purified by recrystallization using THF and an n-hexane mixed solvent.[30] BLA-NCA, a white powdery substance, was obtained by freeze-drying.

Synthesis of folic acid-poly(ethylene glycol)-poly(β-benzyl-L-aspartate) copolymers. FA-PEG-PBLA copolymers were prepared by ring-opening polymerization of BLA-NCA. BLA-NCA was dissolved in DMF and FA-PEG-NH_2 dissolved in chloroform was added. The quantities of solvents were adjusted to 2 mL of DMF per 1 g of BLA-NCA, with chloroform added at 10 times the DMF concentration. We controlled the molar feed ratio to obtain a series of FA-PEG-PBLA copolymers with PBLA segments of various lengths ranging from 10 to 50 repeat units (Table 1). The reaction was allowed to proceed at 40°C for 48 h in the dark under nitrogen. The reaction mixture was precipitated with excess cold diethyl ether, and the precipitate was collected by centrifugation. The precipitate was dissolved in 1,4-dioxane and freeze-dried.[31] Self-assembled nanoparticles of FA-PEG-PBLA were prepared by a dialysis process as reported previously.[32,33]

Synthesis of FA-PEG-P(Asp-Hyd). To conjugate the photosensitizer onto copolymers through pH-responsive cleavage linkage, the benzyl esters at the side chains of FA-PEG-PBLA were substituted with hydrazide groups. FA-PEG-PBLA (160 mg; 0.11 mmol) was dissolved in DMSO (5 mL). Then, hydrazine monohydrate (281 μL; 5.7 mmol) (10-fold excess of hydrazine monohydrate relative to benzyl groups) was added. The reaction was stirred at 1000 r/min for 4 h at room temperature in the dark, diluted with 2 mL deionized water, and the product was purified by dialysis against deionized water followed by freeze-drying.[34]

Conjugation of 2,4-diacetyl deuteroporphyrin IX dimethyl ether (DD-PpIX) to FA-PEG-P(Asp-Hyd) through pH-sensitive linkage. DD-PpIX (19.8 mg; 31.8 mmol) was dissolved in DMF (10 mL). FA-PEG-P(Asp-Hyd) (20.4 mg; 0.002 mmol) was dissolved in acetic acid (1 mL) and added slowly to the DD-PpIX solution. The reaction mixture was stirred at 500 r/min for 24 h at room temperature in the dark. The mixture was precipitated with an excess of cold diethyl ether, and the precipitate was collected by centrifugation. The precipitate was washed several times with THF and collected by centrifugation until the supernatant was colorless. In addition, FA-PEG-P(Asp-Hyd)-DD-PpIX copolymers were

Table 1. The size of FA-PEG-PBLA polymeric nanoparticles depending on hydrophobic segment length.

Samples[a]	Feed ratio[b] (molar ratio)	Copolymer composition[c] (molar ratio)	Molecular weight (g/mol)[c]		Size[d] (nm)	Polydispersity index[d]
			Hydrophilic segment	Hydrophobic segment		
FA-PEG-$PBLA_{10}$	1:10	1:9.8	3791.4	2009	105.3 ± 4.2	0.246 ± 0.016
FA-PEG-$PBLA_{20}$	1:20	1:19.5	3791.4	3998	108.3 ± 3.8	0.224 ± 0.018
FA-PEG-$PBLA_{30}$	1:30	1:28.3	3791.4	5802	109.5 ± 3.5	0.162 ± 0.021
FA-PEG-$PBLA_{40}$	1:40	1:39.6	3791.4	8118	113.0 ± 4.3	0.147 ± 0.013
FA-PEG-$PBLA_{50}$	1:50	1:50.0	3791.4	10250	124.6 ± 3.2	0.271 ± 0.015

[a]FA-PEG-$PBLA_n$ copolymer; n, number of BLA units.
[b]The molar feed ratio of FA-PEG-NH_2 to BLA-NCA.
[c]Molar composition of copolymer, determined by ^1H NMR with DMSO-d_6 as solvent (PEG to BLA units).
[d]Determined by DLS.

Table 2. The size of FA-PEG-P(Asp-Hyd)$_{50}$-DD-PpIX polymeric nanoparticles depending on DD-PpIX conjugating content.

Sample[a]	Feed ratio[b] (weight ratio)	Drug conjugating contents[c] (DCC) (%)	Molecular weight (g/mol)[c]		Size[d] (nm)	Polydispersity index[d]
			Hydrophilic segment	Hydrophobic segment		
FA-PEG-P(Asp-Hyd)$_{50}$-DD-PpIX$_{0.3}$	0.30:1	12.3	10241.4	1432	298.0 ± 9.2	0.337 ± 0.011
FA-PEG-P(Asp-Hyd)$_{50}$-DD-PpIX$_{0.5}$	0.50:1	21.9	10241.4	2864	222.2 ± 4.3	0.174 ± 0.014
FA-PEG-P(Asp-Hyd)$_{50}$-DD-PpIX$_{0.75}$	0.75:1	26.4	10241.4	3674	219.8 ± 3.6	0.264 ± 0.016
FA-PEG-P(Asp-Hyd)$_{50}$-DD-PpIX$_{1.0}$	1.00:1	37.6	10241.4	6164	181.0 ± 2.4	0.175 ± 0.017

[a]FA-PEG-P(Asp-Hyd)$_n$-DD-PpIX$_m$ is 2,4-diacetyl deuteroporphyrin IX dimethyl ether (DD-PpIX)-conjugated in copolymers. n, number of BLA units; m, weight feed ratio of DD-PpIX to copolymer.
[b]Weight feed ratio of DD-PpIX to copolymer.
[c]Determined by ^{1}H NMR using DMSO-d_6 and $CDCl_3$ as solvent.

$$\text{DCC}\,(\%) = \frac{\text{Amount of DD} - \text{Pp IX in nanoparticle}}{\text{Amount of DD} - \text{Pp IX conjugatednanoparticle}} \times 100\% = \frac{\text{DD} - \text{Pp IX}}{\text{DD} - \text{Pp IX} + \text{Copolymer}} \times 100\%$$

[d]Determined by DLS.

prepared by varying the weight feed ratio of DD-PpIX to copolymer over a range of 0.3–1.0, as shown in Table 2. The procedure for the synthesis of FA-PEG-P(Asp-Hyd)-DD-PpIX copolymers is illustrated in Figure 1.

FA-PEG-P(Asp-Hyd)-DD-PpIX copolymers with pH-sensitive linkages were dissolved in DMSO followed by dialysis against $NaHCO_3$ (pH 8.0) for 3 days to achieve nanoparticle formation. The product was freeze-dried and analyzed by ^{1}H NMR in order to calculate the drug conjugating content (DCC).

$$\text{DCC}\,(\%) = \frac{\text{Amount of DD} - \text{Pp IX in nanoparticle}}{\text{Amount of DD} - \text{Pp IX conjugated nanoparticle}} \times 100\% = \frac{\text{DD} - \text{Pp IX}}{\text{DD} - \text{Pp IX} + \text{Copolymer}} \times 100\%$$

Preparation and characterization of self-assembled nanoparticles

The compositions and molecular weights of the copolymers were determined by 400 MHz ^{1}H NMR (JNM-AL400, JEOL, Tokyo, Japan) using D_2O, DMSO-d_6, $CDCl_3$ as the solvent. The sizes and size distributions of the nanoparticles were determined by dynamic light scattering (DLS) (ELS-Z, OTSUKA, Japan) at 25°C using a He-Ne laser (633 nm) as a light source.[10,23,35] The scattered light was measured at 90° and collected by the autocorrelator. The morphologies of the nanoparticles were determined by field emission scanning electron microscopy (FE-SEM) (JSM-7000F, JEOL, Tokyo, Japan) at 15 kV.

In vitro test of DD-PpIX release from the nanoparticles

In vitro testing of DD-PpIX release from FA-PEG-P(Asp-Hyd)-DD-PpIX nanoparticles was performed using a dialysis diffusion method. The pH-dependent release properties were determined in acetate buffer (pH 5.0) and phosphate-buffered saline (PBS) (pH 7.4) at 37°C. First, 3 mg of FA-PEG-P(Asp-Hyd)$_{50}$-DD-PpIX nanoparticles were dispersed in 3 mL of medium and placed in a dialysis bag with a molecular weight cut-off of 2 kDa. Dialysis bags were immersed in 35 mL of release medium and kept in a shaking water bath at 37°C with stirring (120 r/min). At indicated time intervals, the dialysis bags were removed and placed into fresh release medium (35 mL). The used release medium was freeze-dried and the powder was dissolved in DMF followed by centrifugation to remove the salt. The amount of released DD-PpIX was analyzed by UV-visible spectrophotometry (UVmini-1240, Shimadzu, Japan) at a wavelength of 418 nm.

Cellular uptake of DD-PpIX-conjugated nanoparticles

HeLa cells (1×10^4 cells/well) were seeded onto 96-well plates and cultured in RPMI 1640 containing 10% FBS, and 1% penicillin–streptomycin at 37°C in a humidified 5% CO_2 and 95% air atmosphere. After 24 h, the medium was replaced with 100 μL of fresh medium containing free DD-PpIX (10 μg/mL) or FA-PEG-P(Asp-Hyd)$_{50}$-DD-PpIX$_{1.0}$ nanoparticles (10 μg/mL DD-PpIX equivalent) and then incubated

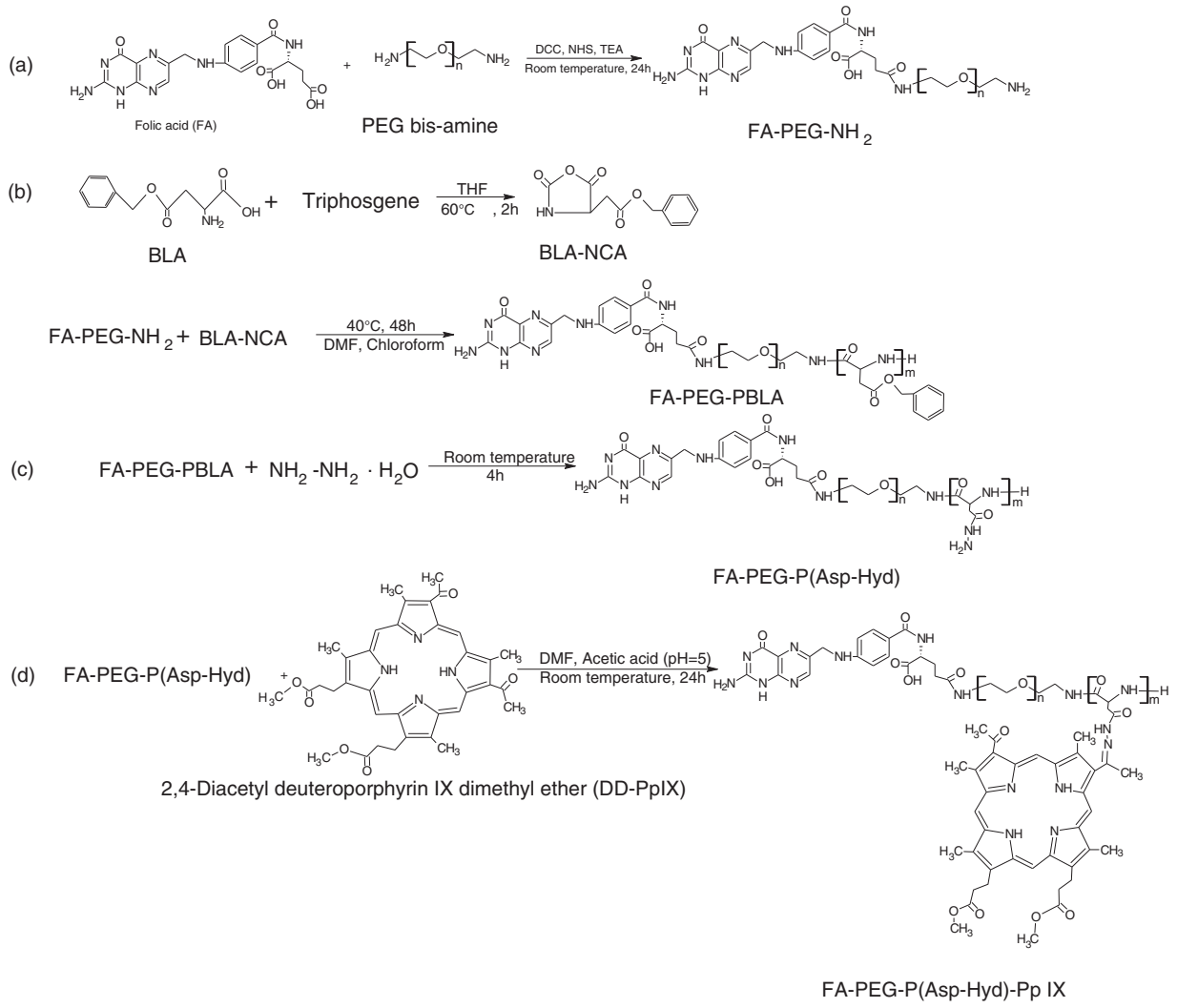

Figure 1. Synthesis of: (a) folic acid-conjugated PEG (FA-PEG-NH_2); (b) folic acid-conjugated amphiphilic PEG-PBLA copolymers (FA-PEG-PBLA); (c) FA-PEG-P(Asp-Hyd); and (d) FA-PEG-P(Asp-Hyd)-DD-PpIX.

for 4 h. (Water-insoluble free DD-PpIX was dissolved in DMSO and then diluted in culture medium until the DMSO concentration reached<0.1%.)[26] The cells were washed with PBS and harvested using 0.05% trypsin-EDTA. 4′,6-Diamidine-2-phenylindol (DAPI) solution was added to stain the cell nucleus at room temperature. All experiments were carried out in a dark room to prevent photodegradation of the probes. The cells were visualized using a Zeiss LSM 510 confocal laser scanning microscope (Carl Zeiss Ltd., Germany).

For the flow cytometry assay, HeLa cells (2×10^5 cells/well) were seeded onto 6-well plates in 1.5 mL RPMI 1640 and allowed to attach for 24 h. After cell attachment, the medium was replaced with 1.5 mL of fresh medium containing free DD-PpIX (10 μg/mL) or FA-PEG-P(Asp-Hyd)$_{50}$-DD-PpIX$_{1.0}$ nanoparticles (10μg/mL DD-PpIX equivalent) and then incubated for 4 h. Then the cells were washed with PBS and cells were trypsinized. The harvested cells were washed with cold PBS and fixed using 4% paraformaldehyde solution. After fixation, the sample was washed again using PBS, and the cellular fluorescence was quantified by FACSCAN flow cytometry (BD Biosciences, USA). The DD-PpIX fluorescence was excited by laser at 633 nm.

In vitro phototoxicity test of DD-PpIX-conjugated nanoparticles

HeLa cells (1×10^4 cells/well) were seeded onto 96-well plates in 100 μL RPMI 1640 and allowed to attach for 24 h. After cell attachment, the medium was replaced with 100 μL of fresh medium containing free DD-PpIX

(10 μg/mL) or FA-PEG-P(Asp-Hyd)$_{50}$-DD-PpIX$_{1.0}$ nanoparticles (10 μg/mL DD-PpIX equivalent) and then incubated for 4 h. The cells were washed with PBS and replaced with fresh culture medium. The samples were irradiated at 0.4 mW/cm^2 with a He-Ne laser (670 nm) for 0, 15, 30 min. Then, irradiated cells were incubated at 37°C for 24 h and cell viability was evaluated using a Cell Counting Kit 8 (CCK-8, Dojindo Laboratories, Japan). Untreated cells were considered to be 100% viable cells. Dark-toxicities of the free DD-PpIX and FA-PEG-P(Asp-Hyd)$_{50}$-DD-PpIX$_{1.0}$ nanoparticles were also evaluated by incubation for 4 h at the same DD-PpIX concentration without laser irradiation.

Results and discussion

Synthesis and characterization of FA-PEG-PBLA-based copolymers

We confirmed the synthesis of intermediates at each step and the final product, FA-PEG-P(Asp-Hyd)-DD-PpIX copolymers, using ^{1}H NMR. Results are shown in Figure 2 and Table 1.

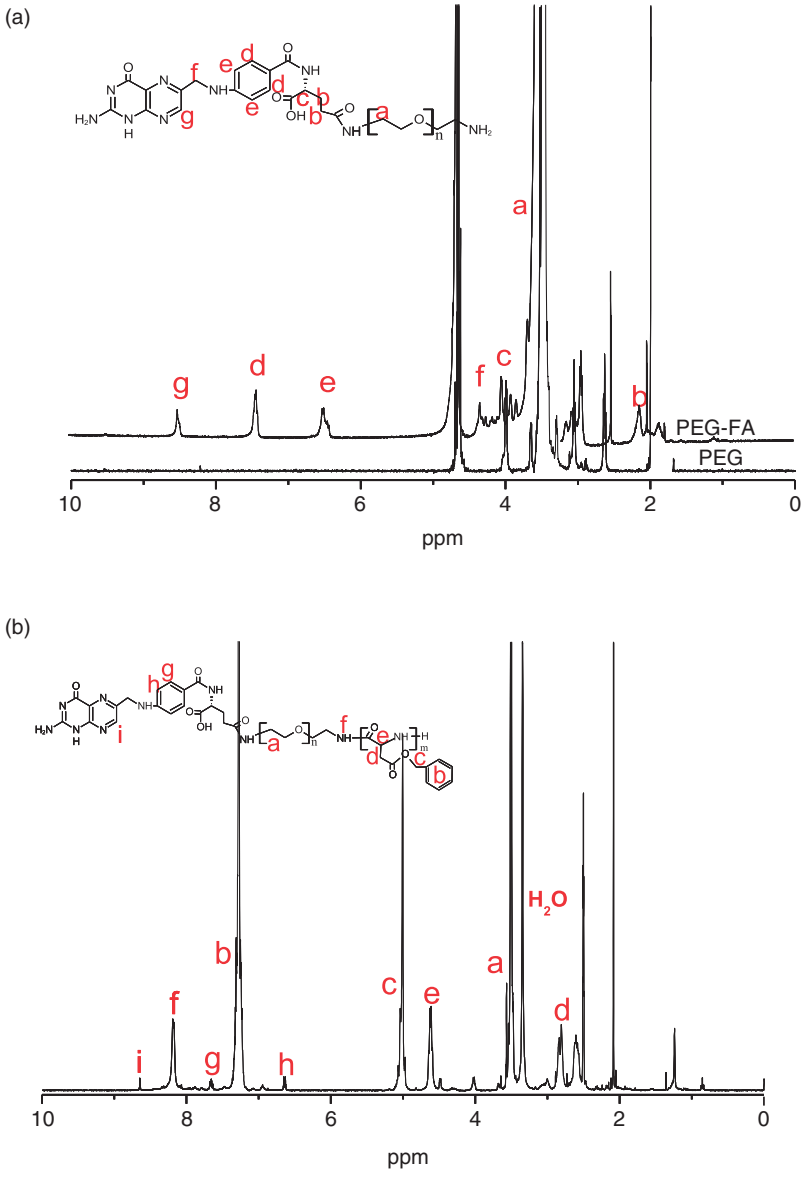

Figure 2. ^{1}H NMR spectra of: (a) FA-PEG-NH$_2$; (b) FA-PEG-PBLA; (c) FA-PEG-P(Asp-Hyd); and (d) FA-PEG-P(Asp-Hyd)-DD-PpIX.

The procedure for the synthesis of FA-PEG-P(Asp-Hyd)-DD-PpIX copolymers is illustrated in Figure 1. First, to introduce FA ligands to copolymers for tumor targeting, FA-conjugated PEG was prepared by reactions of the amino group of PEG-bis(amine) with the FA carboxyl group (Figure 1(a)). The ^{1}H NMR spectrum of the resulting FA-PEG-NH_2 conjugate is shown in Figure 2(a), with a peak of about 3.5 ppm corresponding to the methylene proton of PEG, and the peaks at 6.5 ppm, 7.4 ppm, and 8.5 ppm corresponding to the protons of C_e, C_d, and C_g in FA. The composition of FA in the conjugate can be calculated from the relative intensity ratio of the methylene proton of PEG at 3.5 ppm and the proton of the C_g of FA at 8.5 ppm. In order to get FA-PEG-NH_2, we control the molar feed ratio of FA to PEG-bis(amine) at 1.2:1.

FA-PEG-PBLA block copolymers were synthesized by ring-opening polymerization of β-benzyl-L-aspartate N-carboxy anhydride (BLA-NCA) using the end amino group of FA-PEG-NH_2 in a DMF-chloroform solvent as an initiator (Figure 1(b)). As shown in Figure 2(b), the structure of FA-PEG-PBLA was confirmed by peaks at 5.1 ppm and 7.3 ppm that correspond to the methylene protons and the PBLA side chain benzyl group. The peak at 8.2 ppm corresponds to secondary amine protons in the PBLA main chain. In addition, FA-PEG-PBLA amphiphilic copolymers with various compositions were synthesized by varying

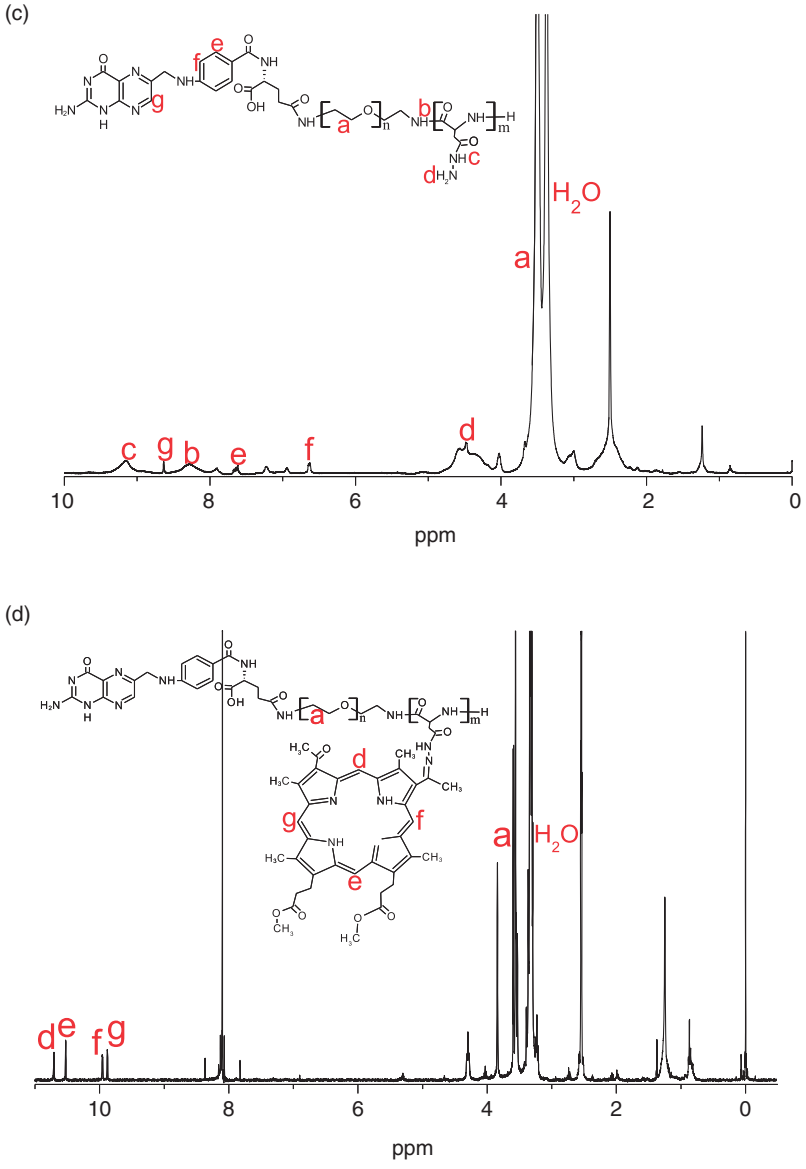

Figure 2. ^{1}H NMR spectra of: (a) FA-PEG-NH_2; (b) FA-PEG-PBLA; (c) FA-PEG-P(Asp-Hyd); and (d) FA-PEG-P(Asp-Hyd)-DD-PpIX.

the feed molar ratio of BLA-NCA to FA-PEG-NH_2 as shown in Table 1. From the ^{1}H NMR spectrum, we determined the number of repeat units in PBLA by calculating the relative intensity ratio of the PEG chain methylene proton (–OCH_2CH_2–, 3.5 ppm) to the methylene proton near the benzyl group of the PBLA chain (–$CH_2C_6H_5$, 5.1 ppm).

In the next step, FA-PEG-P(Asp-Hyd) copolymers with reactive hydrazide groups were prepared by a simple reaction of hydrazine monohydrate with the benzyl groups of the FA-PEG-PBLA block copolymer (Figure 1(c)). An excess of hydrazine monohydrate was used to avoid cross-linking or branching of the polymer. The composition of FA-PEG-P(Asp-Hyd) was confirmed by comparisons to ^{1}H NMR spectra (Figure 2(b) and (c)). In Figure 2(c), the peaks at 5.1 ppm and 7.3 ppm corresponding to the methylene protons and PBLA side chain benzyl group disappeared, but peaks at 4.4 ppm and 9.2 ppm are present. These are the protons of the hydrazide groups, and indicate that the benzyl groups were successfully substituted by hydrazide groups.

In the final step, the DD-PpIX was conjugated to the hydrazide groups of FA-PEG-P(Asp-Hyd) through pH-sensitive hydrazone linkage via an acetic acid-catalyzed reaction (Figure 1(d)). Conjugation was confirmed by the presence of characteristic peaks of DD-PpIX at 9.8 ppm, 9.9 ppm, 10.5 ppm, and 10.7 ppm, and characteristics peaks of FA, PEG and PBLA, as shown in Figure 2(d).

The DCC was confirmed by ^{1}H NMR using the relative intensity ratio of the methylene protons of the PEG chain (–OCH_2CH_2–, 3.5 ppm) to the methylene protons of DD-PpIX (9.8 ppm, 9.9 ppm, 10.5 ppm and 10.8 ppm).

Micellar properties of FA-PEG-PBLA and FA-PEG-P(Asp-Hyd)-DD-PpIX copolymers

Size and stability are key properties that influence in vivo performance for drug delivery by nanocarrier-polymeric nanoparticles. These two factors affect the biodistribution and circulation time of drug carriers. Stable and smaller particles exhibit reduced uptake by the RES and provide efficient passive tumor-targeting ability via an EPR effect.[36]

FA-PEG-PBLA and FA-PEG-P(Asp-Hyd)-DD-PpIX copolymers form nanoparticles with core/shell architecture during dialysis in aqueous solutions because of their amphiphilicity. We examined the size, size distribution, and morphology of FA-PEG-PBLA and FA-PEG-P(Asp-Hyd)-DD-PpIX nanoparticles by DLS and FE-SEM.

Figure 3(a) shows the typical size distribution of FA-PEG-$PBLA_{50}$ copolymeric nanoparticles. DLS measurements showed an average size of 124 nm, and the size distribution exhibited a narrow and monodisperse unimodal pattern. Table 1 outlines the sizes of FA-PEG-PBLA polymeric nanoparticles with different lengths of hydrophobic PBLA. The sizes of amphiphilic copolymeric nanoparticles affect molecular weight and intermolecular interactions.[37,38] The particle size of the FA-PEG-PBLA copolymeric nanoparticles ranged from 105 to 124 nm (Table 1). Nanoparticle size gradually increased as the molecular weight of FA-PEG-PBLA and the hydrophobic PBLA segment increased.

Figure 3(b) shows a typical size distribution of PS-conjugated FA-PEG-$(Asp\text{-}Hyd)_{50}$-DD-$PpIX_1$ nanoparticles. According to DLS, the average size was 181 nm, larger than the size before PS conjugating. The size

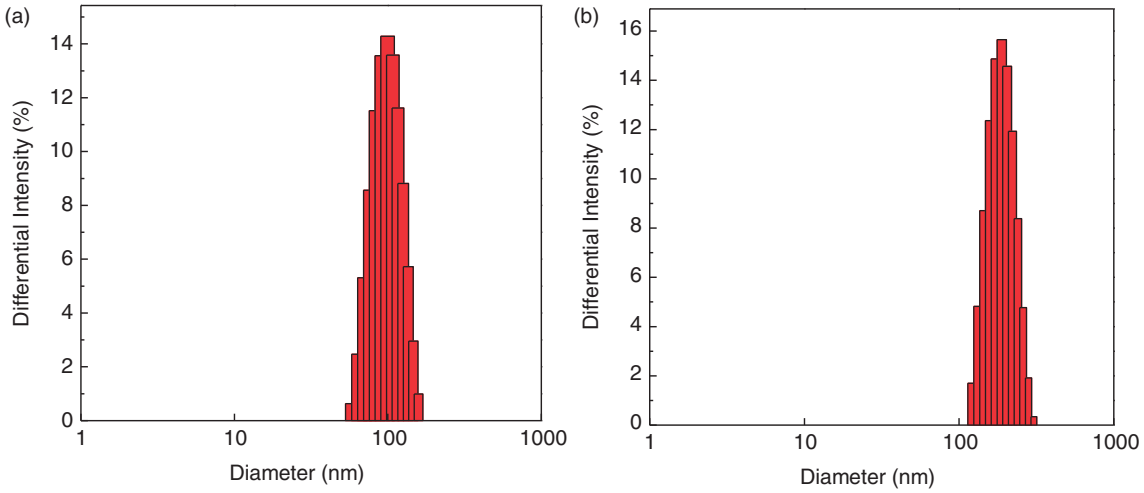

Figure 3. Typical size distributions of: (a) FA-PEG-$PBLA_{50}$; and (b) FA-PEG-$P(Asp\text{-}Hyd)_{50}$-DD-$PpIX_{1.0}$.

distribution was very close to the narrow distribution seen before PS conjugating. Table 2 shows the sizes of FA-PEG-P(Asp-Hyd)$_{50}$-DD-PpIX polymeric nanoparticles with different PS contents. Nanoparticle size decreased with increased DD-PpIX content. As hydrophobic DD-PpIX content increased, hydrophobic interactions between DD-PpIX in the cores of the PEG-P(Asp-Hyd)$_{50}$-DD-PpIX nanoparticles was enhanced. This increased the density of the nanoparticle cores, thereby decreasing nanoparticle size.

The morphologies of FA-PEG-PBLA$_{50}$ and FA-PEG-(Asp-Hyd)$_{50}$-DD-PpIX$_1$ were evaluated by FE-SEM. As shown in Figure 4, FA-PEG-PBLA$_{50}$ and FA-PEG-(Asp-Hyd)$_{50}$-DD-PpIX$_1$ nanoparticles were submicron in size and nearly spherical. No aggregation between nanoparticles was observed by FE-SEM.

In vitro DD-PpIX release study

The in vitro release of DD-PpIX from FA-PEG-(Asp-Hyd)$_{50}$-DD-PpIX nanoparticles was investigated under simulated physiological conditions (PBS, pH 7.4) and in an acidic environment (acetate buffer, pH 5.0) at 37°C in order to evaluate the feasibility of using FA-PEG-(Asp-Hyd)-DD-PpIX nanoparticles as PS carriers. Figure 5 shows the amounts of accumulated DD-PpIX released from the FA-PEG-(Asp-Hyd)$_{50}$-DD-PpIX nanoparticles with different DCC values and pH values as a function of time. The DCC-dependent release of DD-PpIX from nanoparticles was observed under both simulated physiological conditions (Figure 5(a)) and in an acidic environment (Figure 5(b)). As the amount of hydrophobic DD-PpIX in FA-PEG-(Asp-Hyd)$_{50}$-DD-PpIX nanoparticles increased, the release rate gradually decreased. This may have been due to high DCC in the nanoparticle cores, which enhanced the hydrophobic interaction between DD-PpIX, slowing the release of DD-PpIX.

For FA-PEG-(Asp-Hyd)$_{50}$-DD-PpIX nanoparticles with the same DCC values, release was strongly dependent on the pH of the medium. DD-PpIX release was much faster at pH 5.0 than at pH 7.4. At pH 5.0, the accumulated amount of released DD-PpIX was 40% after one day; however, the accumulated amount released was only 10% at pH 7.4. Because the pH-sensitive hydrazone bond linker can be hydrolyzed in acidic conditions, DD-PpIX was easily released from FA-PEG-(Asp-Hyd)$_{50}$-DD-PpIX nanoparticles by hydrolysis at pH 5.0. The influence of pH on the release of PS from FA-PEG-(Asp-Hyd)$_{50}$-DD-PpIX nanoparticles suggests that this system could minimize the leakage of free drugs into the circulatory system, and be useful for selective accumulation in solid tumors with release from the carrier.

Cellular localization of DD-PpIX-conjugated nanoparticles

The efficiency of PDT treatment is highly dependent on cellular uptake of PS and accumulation in malignant tissues.[39] The intracellular localizations of free

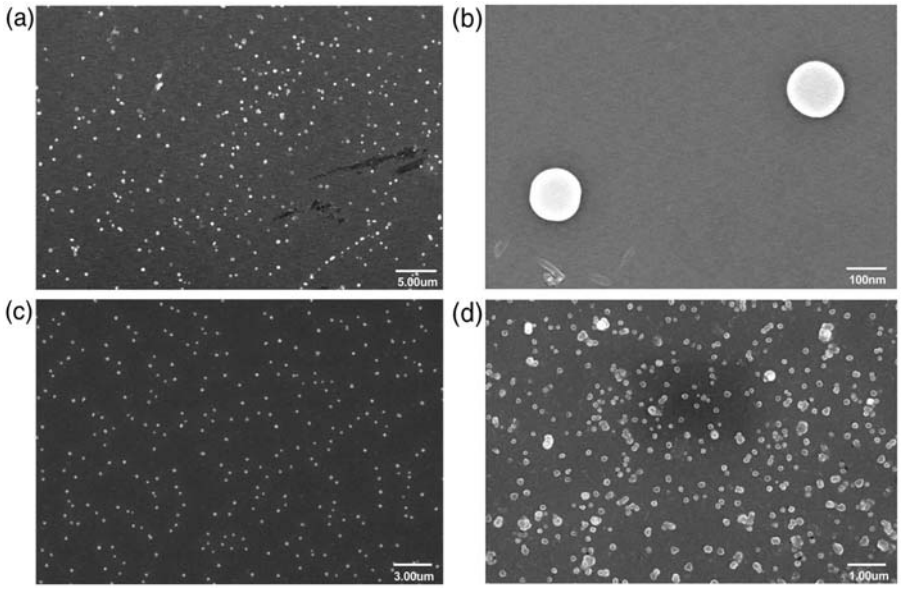

Figure 4. FE-SEM images of: (a) FA-PEG-PBLA$_{50}$ nanoparticles (scale bar = 5.00 μm); (b) FA-PEG-PBLA$_{50}$ nanoparticles (scale bar = 100 nm); (c) FA-PEG-P(Asp-Hyd)$_{50}$-DD-PpIX$_{1.0}$ nanoparticles (scale bar = 3.00 μm); and (d) FA-PEG-P(Asp-Hyd)$_{50}$-DD-PpIX$_{1.0}$ nanoparticles (scale bar = 1.00 μm).

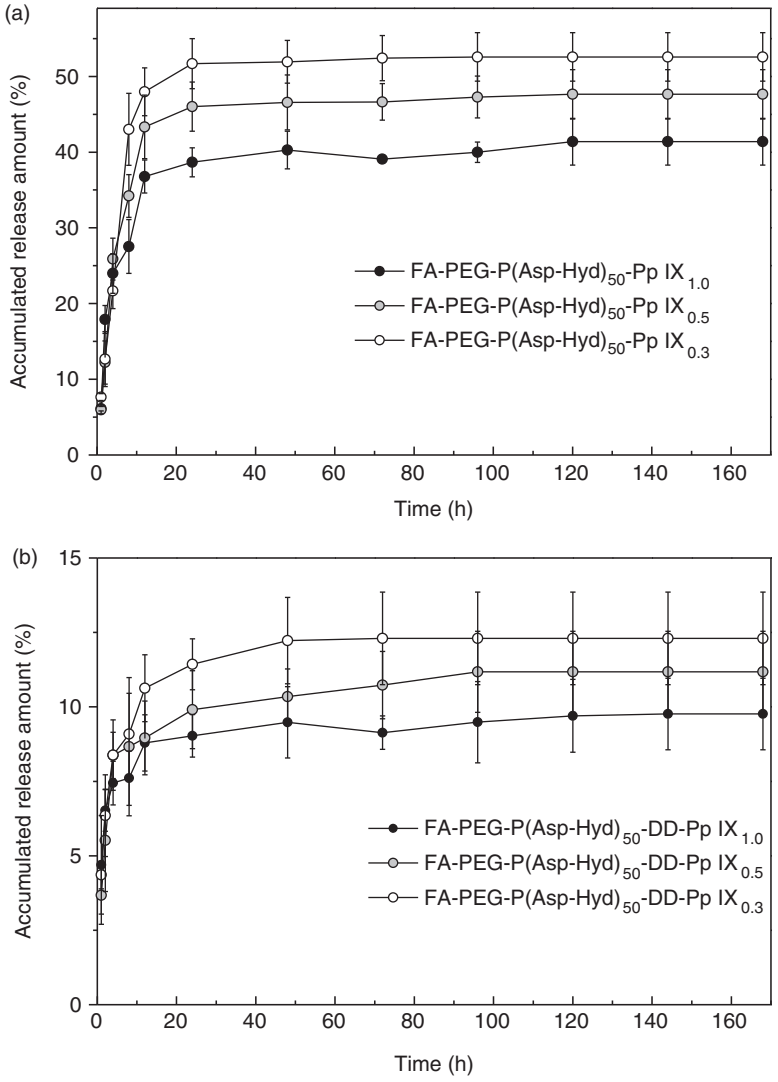

Figure 5. In vitro release behavior of DD-PpIX from FA-PEG-P(Asp-Hyd)-DD-PpIX nanoparticles with different PS conjugating contents and the pH of release medium at: (a) pH 5.0; and (b) pH 7.4.

DD-PpIX and FA-PEG-P(Asp-Hyd)$_{50}$-DD-PpIX$_{1.0}$ nanoparticles in HeLa cells were investigated using flow cytometry and confocal laser scanning microscopy.

Figure 6 shows the flow cytometry assay results. When HeLa cells were incubated with free DD-PpIX, the cellular uptake of free DD-PpIX molecules was about 0.12%. In FA-PEG-P(Asp-Hyd)$_{50}$-DD-PpIX$_{1.0}$ nanoparticles, the cellular uptake was significantly increased (97.25%). The confocal microscopy assay was based on the red fluorescence of DD-PpIX itself and the DAPI blue fluorescence bound to the nucleus (Figure 7). When HeLa cells were incubated with free DD-PpIX and FA-PEG-P(Asp-Hyd)$_{50}$-DD-PpIX$_{1.0}$ nanoparticles, the cellular uptake of DD-PpIX molecules was quite different. For free DD-PpIX, no red fluorescence was detected at the cell membranes (Figure 7(a)). However, treatment of HeLa cells with FA-PEG-P(Asp-Hyd)$_{50}$-DD-PpIX$_{1.0}$ nanoparticles produced strong fluorescence signals from DD-PpIX around the nuclear membrane and the inner parts of the cells (Figure 7(b)), indicating that FA-PEG-P(Asp-Hyd)$_{50}$-DD-PpIX $_{1.0}$ nanoparticles were internalized into the cells.

This result agrees with the results of flow cytometry assays and indicates that DD-PpIX-conjugated nanoparticles with higher water solubility and folate ligands could effectively improve the cellular uptake of hydrophobic DD-PpIX molecules.

In vitro phototoxicity test of DD-PpIX-conjugated nanoparticles

The in vitro phototoxicity of free DD-PpIX and DD-PpIX-conjugated nanoparticles on HeLa cells were compared after treatment with or without laser

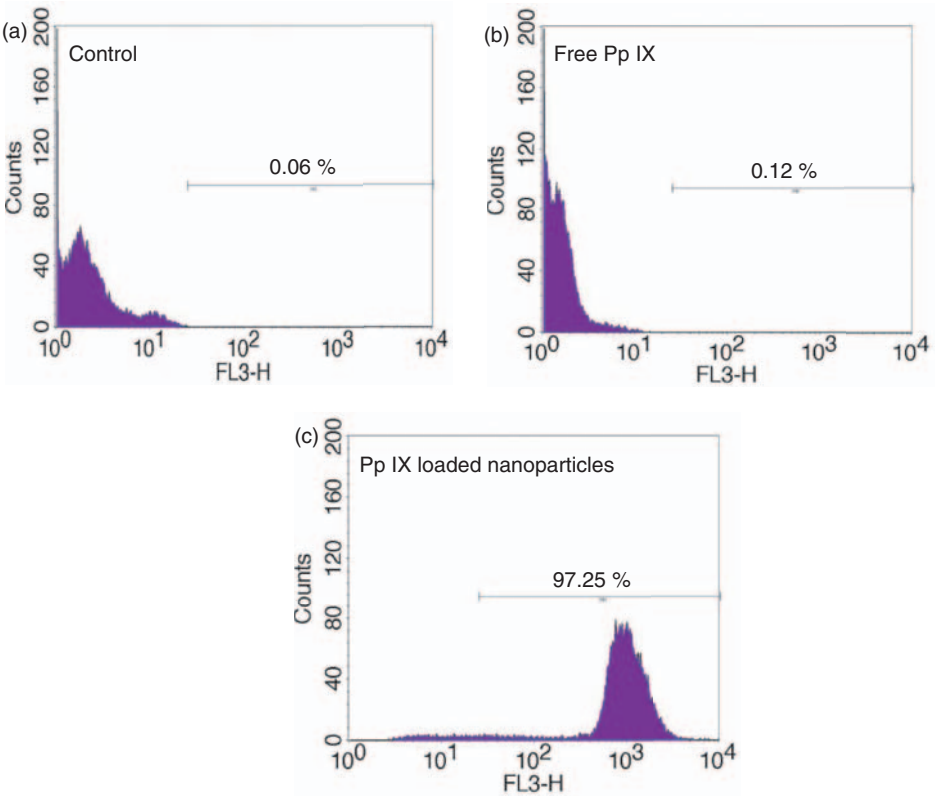

Figure 6. Flow cytometry assays of cellular uptake of free DD-PpIX and DD-PpIX conjugated nanoparticles against HeLa cells: (a) control; (b) free DD-PpIX; and (c) FA-PEG-P(Asp-Hyd)$_{50}$-DD-PpIX$_{1.0}$ nanoparticles.

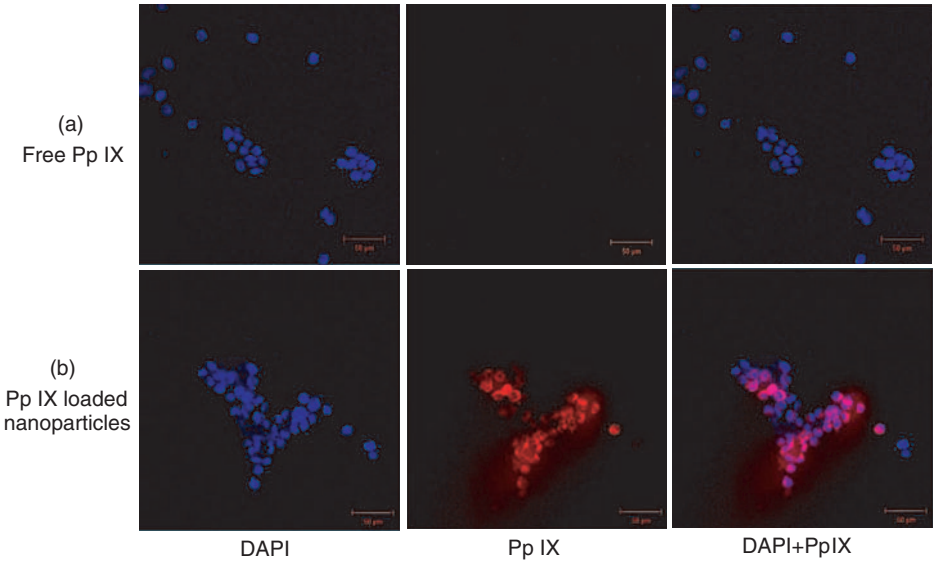

Figure 7. Cellular localization of free DD-PpIX and DD-PpIX-conjugated nanoparticles against HeLa cells observed by confocal laser scanning microscope: (a) free DD-PpIX; and (b) FA-PEG-P(Asp-Hyd)$_{50}$-DD-PpIX$_{1.0}$ nanoparticles [DAPI (blue); DD-PpIX (red)].

irradiation (670 nm, 0.4 mW/cm^2) to determine the PDT efficacy of DD-PpIX-conjugated nanoparticles (Figure 8).

Without laser treatment (0 min), free DD-PpIX and FA-PEG-P(Asp-Hyd)$_{50}$-DD-PpIX$_{1.0}$ nanoparticles exhibited slight dark-toxicity (cell viability: 84.0–97.2%) even at high concentrations of DD-PpIX (10 μg/mL). After irradiation, free DD-PpIX did not show any significant changes in cell viability (100.9% cell viability after 15 min irradiation; 100.2% cell

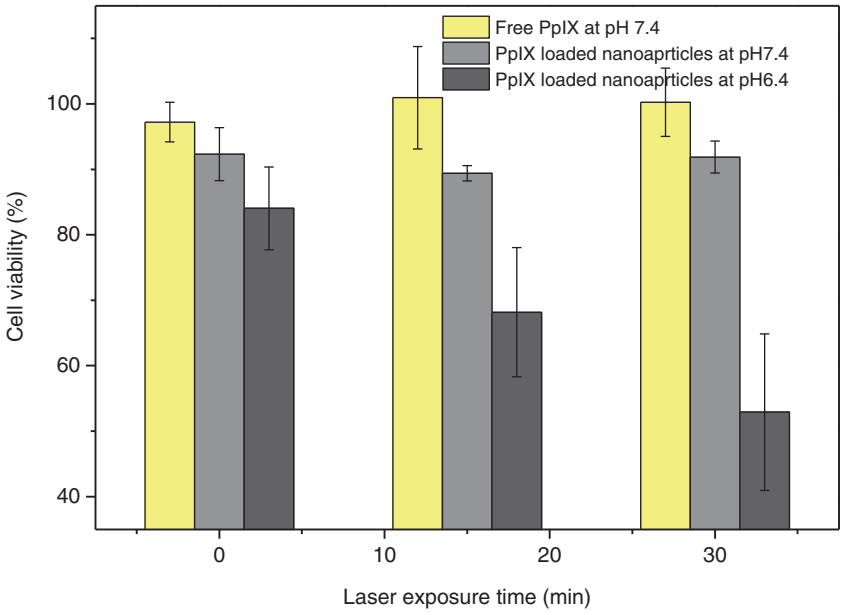

Figure 8. In vitro phototoxicity test using free DD-PpIX and FA-PEG-P(Asp-Hyd)$_{50}$-DD-PpIX$_{1.0}$ nanoparticles against HeLa cells depending on laser exposure time.

viability after 30 min irradiation), probably due to the low water solubility of free DD-PpIX molecules causing DD-PpIX molecules not to be effectively internalized into cells. This result agreed with the results of cellular uptake studies.

For DD-PpIX nanoparticles at pH 7.4, the cell viability was slightly decreased after irradiation compared with free DD-PpIX (Figure 8). However, at pH 6.4, laser treatment drastically decreased cell viability depending on laser exposure time, implying that DD-PpIX-conjugated nanoparticles effectively generated cytotoxic species and induced cell depletion. This result suggests that rapid release of DD-PpIX from nanoparticles containing pH-sensitive hydrazone linkages under weakly acidic extracellular conditions can enhance phototoxicity effects compared with effects at physiological pH.

Conclusions

A tumor-targeting ligand-conjugated nanoparticle carrier with the potential to function as a pH-responsive release reservoir was designed for targeted PS delivery in PDT. FA-conjugated amphiphilic block copolymers of FA-PEG-PBLA were synthesized with various molecular weights and hydrophobic chain lengths. DD-PpIX was conjugated to the hydrophobic segment through pH-sensitive hydrazone bonds. FA-PEG-PBLA and FA-PEG-P(Asp-Hyd)$_{50}$-DD-PpIX with pH-sensitive linkages formed self-assembled nanoparticles in aqueous solution. DLS and FE-SEM measurements indicated that the nearly spherical nanoparticles had a narrow size distribution with a mean diameter of 124 nm for FA-PEG-PBLA and 181 nm for FA-PEG-P(Asp-Hyd)$_{50}$-DD-PpIX$_{1.0}$. These stable nanoparticles are suitable for triggering the EPR effect. The release of DD-PpIX from FA-PEG-P(Asp-Hyd)$_{50}$-DD-PpIX$_{1.0}$ nanoparticles was significantly influenced by the conjugating contents of PS and the pH of the medium. In particular, DD-PpIX release was faster at pH 5.0 than at pH 7.4 due to hydrolysis of hydrazone linkages in acidic conditions. The cellular uptake and in vitro phototoxicity test results indicated that FA-PEG-(Asp-Hyd)-DD-PpIX nanoparticles had low dark-toxicity and effectively induced the destruction of cancer cells under weakly acidic tumoral conditions. These results suggest that the FA-PEG-(Asp-Hyd)-DD-PpIX nanoparticle system has potential for use as an effective PS delivery system for PDT applications.

Funding

This research was supported by Basic Science Research Program through the National Research Foundation of Korea (NRF) funded by the Ministry of Education, Science and Technology (2012013658). This work was partially supported by the National Research Foundation of Korea (NRF) grant funded by the Korea government (MEST) (20110030590).

References

1. Levy JG and Obochi M. New applications in photodynamic therapy introduction. *Photochem Photobiol* 1996; 64: 737–739.
2. Dolmans DEJGJ, Fukumura D and Jain RK. Photodynamic therapy for cancer. *Nat Rev Cancer* 2003; 3: 380–387.
3. Ackroyd R, Kelty C, Brown N, et al. The history of photodetection and photodynamic therapy. *Photochem Photobiol* 2001; 74: 656–669.
4. Dougherty TJ, Gomer CJ and Henderson BW. Photodynamic therapy. *J Natl Cancer Inst* 1998; 90: 889–905.
5. Wilson BC. Photodynamic therapy for cancer: principles. *Can J Gastroenterol* 2002; 16: 393–396.
6. Dougherty TJ. Photosensitizers: therapy and detection of malignant tumors. *Photochem Photobiol* 1987; 45: 879–889.
7. Allison RR, Cuenca RE, Downie GH, et al. Clinical photodynamic therapy of head and neck cancers-a review of applications and outcomes. *Photodiag Photodyn Therap* 2005; 2: 205–222.
8. DeRosa MC and Crutchley RJ. Photosensitized singlet oxygen and its applications. *Coordinat Chem Rev* 2002; 233–234: 351–371.
9. Konan YN, Gurny R and Allemann E. State of the art in the delivery of photosensitizers for photodynamic therapy. *J Photochem Photobiol B: Biol* 2002; 66: 89–106.
10. Li BH, Moriyama EH, Li FG, et al. Diblock copolymer micelles deliver hydrophobic protoporphyrin IX for photodynamic therapy. *Photochem Photobiol* 2007; 83: 1505–1512.
11. Woodburn K and Kessel D. The alteration of plasma-lipoproteins by cremophor EL. *J Photochem Photobiol B-Biol* 1994; 22: 197–201.
12. Ferro S, Ricchelli F, Mancini G, et al. Inactivation of methicillin-resistant staphylococcus aureus (MRSA) by *liposome-delivered photo sensitising agents*. *J Photochem Photobiol B-Biol* 2006; 83: 98–104.
13. Kim HS, Lee HJ, Lee DJ, et al. Asymmetric total syntheses of (+)-3-(Z)-laureatin and (+)-3-(Z)-isolaureatin by "lone pair−lone pair interaction-controlled" isomerization. *J Am Chem Soc* 2007; 129: 2269–2275.
14. Hone DC, Walker PI, Gowing RE, et al. Generation of cytotoxic singlet oxygen via phthalocyanine-stabilized gold nanoparticles: a potential delivery vehicle for photodynamic therapy. *Langmuir* 2002; 18: 2985–2987.
15. Ideta R, Tasaka F, Jang WD, et al. Nanotechnology-based photodynamic therapy for neovascular disease using a supramolecular nanocarrier loaded with a dendritic photosensitizer. *Nano Lett* 2005; 5: 2426–2431.
16. Zhang GD, Harada A, Nishiyama N, et al. Polyion complex micelles entrapping cationic dendrimer porphyrin: effective photosensitizer for photodynamic therapy of cancer. *J Control Release* 2003; 93: 141–150.
17. Maeda H. The enhanced permeability and retention (epr) effect in tumor vasculature: the key role of tumor-selective macromolecular drug targeting. *Adv Enzyme Regulat* 2001; 41: 189–207.
18. Bae YS, Nishiyama N, Fukushima S, et al. Preparation and biological characterization of polymeric micelle drug carriers with intracellular pH-triggered drug release property: tumor permeability, controlled subcellular drug distribution, and enhanced in vivo antitumor efficacy. *Bioconj Chem* 2005; 16: 122–130.
19. Gaucher G, Dufresne MH, Sant VP, et al. Leroux, block copolymer micelles: preparation, characterization and application in drug delivery. *J Control Release* 2005; 109: 169–188.
20. Jones MC and Leroux JC. Polymeric micelles - a new generation of colloidal drug carriers. *Eur J Pharm Biopharm* 1999; 48: 101–111.
21. Kale AA and Torchilin VP. Design, synthesis, and characterization of pH-sensitive PEG-PE conjugates for stimuli-sensitive pharmaceutical nanocarriers: the effect of substitutes at the hydrazone linkage on the pH stability of PEG-PE conjugates. *Bioconjug Chem* 2007; 18: 363–370.
22. Huang IP, Sun SP, Cheng SH, et al. Enhanced chemotherapy of cancer using pH-sensitive mesoporous silica nanoparticles to antagonize P-glycoprotein mediated drug resistance. *Molecular Cancer Therap* 2011; 10: 761–769.
23. Knop K, Mingotaud AF, Akra NE, et al. Monomeric pheophorbide (a)-containing poly(ethyleneglycol-b-ε-caprolactone) micelles for photodynamic therapy. *Photochem Photobiol Sci* 2009; 8: 396–404.
24. Shmeeda H, Mak L, Tzemach D, et al. Intracellular uptake and intracavitary targeting of folate conjugated liposomes in a mouse lymphoma model with up-regulated folate receptors. *Molecular Cancer Therapeut* 2006; 5: 818–824.
25. Elnakat H and Ratnam M. Distribution, functionality and gene regulation of folate receptor isoforms: implications in targeted therapy. *Adv Drug Deliv Rev* 2004; 56: 1067–1084.
26. Geszke M, Murias M, Balan L, et al. Folic acid-conjugated core/shell ZnS:Mn/ZnS quantum dots as targeted probes for two photon fluorescence imaging of cancer cells. *Acta Biomater* 2011; 7: 1327–1338.
27. Yoo HS and Park TG. Folate receptor targeted biodegradable polymeric doxorubicin micelles. *J Control Release* 2004; 96: 273– 283.
28. Zhao HZ and Yung LYL. Selectivity of folate conjugated polymer micelles against different tumor cells. *Int J Pharmaceut* 2008; 349: 256–268.
29. Lee RJ and Philip S. Low, folate-mediated tumor cell targeting of liposome-entrapped doxorubicin in vitro. *Biochim Biophys Acta* 1995; 1233: 134–144.
30. Prabaharan M, Grailer JJ, Pilla S, et al. Amphiphilic multi-arm-block copolymer conjugated with doxorubicin via pH-sensitive hydrazone bond for tumor-targeted drug delivery. *Biomaterials* 2009; 30: 5757–5766.
31. Yokoyama M, Kwon GS, Okano T, et al. Preparation of micelle-forming polymer-drug conjugates. *Bioconjug Chem* 1992; 3: 295–301.
32. La SB, Okano T and Kataoka K. Preparation and characterization of the micelle-forming polymeric drug indomethacin-incorporated poly(ethylene oxide) poly(β-benzyl L-aspartate) block copolymer micelles. *J Pharmaceut Sci* 1996; 85: 85–90.

33. Li L, Huh KM, Lee YK, et al. Design of a multifunctional heparin-based nanoparticle system for anticancer drug delivery. *Macromol Res* 2010; 18: 153–161.
34. Akamatsu K, Yamasaki Y, Nishikawa M, et al. Development of a hepatocyte-specific prostaglandin E_1 polymeric prodrug and its potential for preventing carbon tetrachloride-induced fulminant hepatitis in mice. *J Pharmacol Exp Therapeut* 1999; 290: 1242–1249.
35. Bae BC and Na K. Self-quenching polysaccharide-based nanogels of pullulan/folate-photosensitizer conjugates for photodynamic therapy. *Biomaterials* 2010; 31: 6325–6335.
36. Schmalenberg KE, Frauchiger L, Nikkhouy-Albers L, et al. Cytotoxicity of a unimolecular polymeric micelle and its degradation products. *Biomacromolecules* 2001; 2: 851–855.
37. Kim SY and Lee YM. Taxol-loaded block copolymer nanospheres composed of methoxy poly(ethylene glycol) and poly(ε-caprolactone) as novel anticancer drug carriers. *Biomaterials* 2001; 22: 1697–1704.
38. Wu QH, Liang F, Wei TZ, et al. Synthesis and micellization of an amphiphilic biodegradable β-cyclodextrin/poly (γ-benzyl L-glutamate) copolymer. *J Polym Res* 2010; 17: 183–190.
39. Nawalany K, Rusin A, Kepczynski M, et al. Comparison of photodynamic efficacy of tetraarylporphyrin pegylated or encapsulated in liposomes: in vitro studies. *J Photochem Photobiol B: Biol* 2009; 97: 8–17.